IOSR Journal of Environmental Science, Toxicology and Food Technology (IOSR-JESTFT)
e-ISSN: 2319-2402,p- ISSN: 2319-2399.Volume 13, Issue 8 Ser. I (August. 2019), PP 28-43
www.iosrjournals.org

Isotherms, kinetics and equilibrium Studies of adsorption of Lead (II) ions from aqueous solutions Using Polymer-Modified Coconut Shell Activated Carbon (MCSAC)

Ogbeide Osareme .M[1], Ezeh Emmanuel .C[2], Okpara Onyedikachi .O[1]
[1](*Department Of Science Laboratory Technology, Federal College Of Agriculture, P.M.B. 7008, Ishiagu, Ebonyi State, Nigeria)*
[2](*Department Of Industrial Chemistry, Enugu State University Of Science and Technology, P.M.B. 01660, Agbani, Enugu, Nigeria)*
Corresponding Author: Ogbeide Osareme .M

Abstract: *Coconut (Cocos nucicera L) shell activated carbon was modified with urea immobilized-polysiloxane, and its potential for the removal of Pb^{2+} from simulated water samples was studied. It was activated physically to generate the modified coconut shell activated carbon (MCSAC). The functional groups and image morphology of the activated carbons were analyzed using Fourier transform infrared (FTIR) spectroscopy and Scanning Electron Microscope (SEM) respectively. Batch adsorption experiment were carried out using available MCSAC adsorbent for the removal of Pb(II) ions from aqueous solutions. The effect of the initial Pb^{2+} concentration, contact time, adsorbent dosage, temperature and pH were experimentally studied in batch mode to evaluate the adsorption capacity, kinetic and equilibrium. Experimental results revealed that optimal adsorption took place at pH 8.0 and high lead (II) concentration 200 mg/l. The uptake process obeyed the pseudo-second-order kinetic expression and was best described by Harkins-Jura isotherm than other models (Langmuir, Freundlich and Temkin) considered. Thus, MCSAC could be employed as low-cost alternative for removal of Pb^{2+} from industrial wastewater.*

Keywords: *Adsorption isotherm, kinetics, lead (II) ions, activated carbon from coconut shell, modification with polymer*

Date of Submission: 03-08-2019 Date of acceptance: 19-08-2019

I. Introduction

In recent years, Heavy metals are considered trace elements because of their presence in trace concentration. They are metallic elements with relatively high density, toxic or poisonous [1], they are naturally occurring non-biodegradable elements that are found in the earth's crust. Their existence has been a menace to the environment and have drawn global concern. Their occurrence and depositions from various manufacturing processes has created a serious environmental issue in the sense that, excessive concentrations of these metals are detrimental and destabilizes the ecosystems through bioaccumulation in organisms, body, and food chain, causing toxic effects on living organisms by metabolic interference and mutagenesis [2]. Toxicity and persistence in the environment are the major risk exhibits by most of these metals and these has also become a major threat to plant, animals and human life, therefore, must be removed from municipal and industrial effluents. Excessive exposure and intake of these metals, including arsenic, nickel, lead, and cadmium, has been associated with various diseases, such as cancer, cardiovascular and neurological diseases [3]. Humans also suffers accumulative poisoning, nervous system damage, lowering of the reproductive activities of organisms, inhibition of growth, as well as death in most living beings.

Apart from the earth's crust, heavy metals are released into the environment by both natural and anthropogenic activities such as milling, mining, smelting operations, industrial activities, domestic and agricultural use of metals and metal compounds. Other sources of heavy metal contamination into the environment are through metal corrosion, atmospheric deposition, soil erosion of metal ions and leaching of heavy metals [4].

Lead is one of the heavy metals considered toxic to humans, animals, fishes and environment. Some of the major sources of lead released into the environment are from metal finishing industries, paint manufacture, electroplating, metallurgical industry, petroleum refining, fuel combustion, photographic materials, lead-acid battery manufacture and drainage from ore and mines [5,6]. Drinking water delivered through lead pipes or pipes joined with lead solder may contain lead [7].

Water contamination or pollution with heavy metals are the major problem militating against the environment, which are caused by the influence of the heavy metal depositions on soil, water and air [8]. It is suffered mostly in the developing and underdeveloped countries. Many methods have been developed for the treatment and removal of heavy metals concentrations. These methods are expensive, time consuming, differ in their efficiency and can generate toxic sludge and some requires higher energy. Some of the methods are chemical precipitation, filtration, ion exchange, reverse osmosis, sedimentation, solvent extraction, ultra-filtration, electrochemical deposition, coagulation and adsorption [8, 26]. However, the above mentioned conventional methods are not economically viable for small and medium size industries due to huge capital required [9]. It is therefore necessary to search for low cost alternative techniques that may be effective, economical and sludge free [10].

According to report by Uddin [11], that for trace metal ions concentration in wastewater, the adsorption process is suitable for their removal because they are highly efficient, effective, cheap, simple, sludge free, ease of operation, insensitive to toxic substances, less environmentally degrading and easy recovery [12, 13]. In this case, activated carbon is preferred and seems to be more viable option for removal of lead from wastewater. Activated carbon is an amorphous form of elemental carbon prepared from variety of carbonaceous raw materials, including wood, coal or coconut shells. It is unique and effective agent for purification, isolation and recovery of trace materials [14]. With better awareness of the problems associated with lead came increase in research studies related to treatment methods. Many adsorbent from agricultural by-products have been applied for the removal of lead (II) ions such as activated carbon from the precursors; plantain peels [15], palm karnel shell [16], eggshells [17], thevetia neriifolia nutshell [18], rice husk [19], Date pit [20], Nano-silver coated activated carbon [21], Cedar leaf [22], coconut husk [23], coconut shell [24, 25].

Coconut shell is an attractive and economic alternative for the removal of metal ions from waste water. In this work, coconut shell adsorbent was modified with immobilized polysiloxanes, to increase the functional group and improve selective properties of coconut shell to adsorb the heavy metal Pb (II) through the formation of coordination compound between them [26, 27]. The characterization of the modified coconut shell was carried out by analyzing the fourier Transform Infrared Spectrum (FT-IR) and Scanning Electron Microscopy (SEM) of the adsorbent. The aim of this work was to study the adsorption capacity of coconut shell that was modified with inorganic polymer (polysiloxane) for the removal of Pb (II) ions from aqueous solutions. The effects of initial metal ion concentration, contact time, temperature, pH and adsorbent dosage on the adsorption efficiency were also investigated. In addition, the equilibrium data was tested on adsorption isotherms; Freiundlich, Langmuir, temkin and Harkins-Jura models. And kinetic models are applied on experimental data to observe the kinetic behavior of adsorption process. (10)

II. Material And Methods

2.1 Materials and Instruments

All the reagents used in this work was of analytiacal grade; lead nitrate, $Pb(NO_3)_2$ (99 % Labosi, India), NaOH, and HCl. The instruments used was Flame Atomic Absorption Spectrophotometer FS240AA Agilent U.S.A., Buck scientific M530 USA FTIR was used for the analysis, and SEM-Phenom ProX by Phenom World Eindhoven, netherlands.

2.2 Methods

2.2.1 Preparation of Coconut shell activated carbon (CSAC)

The activation process was physical method. Coconut shell was gathered from urban area of Ogbete main market Enugu State. They were thoroughly washed with sponge and clean water severally to remove dirt and after with distilled water. then they were sun dried for 3 days before being finally oven-dried at 105^{o}C for 5hr. The dried shells was weighed and it was 2.3 kg. Then crushed into smaller pieces for easy activation. And was loaded into a heat chamber of electric heat muffle furnace to pyrolyse in the absence of air, at temperature raised to 650^{O}C for 1.30 min, then the furnace was switch off. The substance was kept to cool overnight, after that, the activated carbon was collected, grounded and sieved to fine particles. The weight was 1.15 kg and then stored in air tight container for further use.

$$\% \text{ Yield} = \frac{\text{Weight of the final product}}{\text{Weight of the initial sample}} \text{ X } 100$$

2.2.2 Preparation of urea immobilized polysiloxane

Tetraethoxysilane (20.83g) was mixed with 15 cm^3 of methanol and 9.95 cm^3 of HCl (0.42 g/cm^3) and stirred very well. 3-chloropropyltriethoxsilane was then added to the mixture and stirred. Gelation occurred after few seconds, and the product was allowed to stand for 12 h, at ambient temperature (room temperature) and then dried in an oven at 90^{o}C. The dried product was grounded, sieved, and washed successively with 50 cm^3 portions of 0.025 g/cm^3 NaOH, water, methanol and diethylether. It was dried again in an oven at 90^{o}C for 10 h.

The product (1.0g) was refluxed with 0.98 g of urea in 50 cm^3 of toluene at 110^oC for 10 h. After which, it was allowed to cool, filtered, and washed with equal portion of 50 cm^3 water, methanol, and diethyl ether, and dried at 90^oC and 1 atm. for 10 h [28].

2.2.3 Modification of activated carbon (CSAC) with urea immobilized polysiloxane

0.5g of the prepared urea immobilized polysiloxane was added to small quantity of de-ionized water. 20g of the activated carbon was added and mixed properly. The mixture was dried in an oven at 50^oC at 150 rpm for about 45 min. After which, the modified coconut shell activated carbon (MCSAC) formed was ready to be used for the adsorption experiments.

2.3 Characterization of the Unmodified and Modified coconut shell activated carbon (MCSAC).

2.3.1 FT-IR Analysis: The CSAC and MCSAC samples were analysed to detect the functional groups present in them using Fourier transform infrared spectroscopy (FTIR). The region of infrared was between 4000 and 600 cm^{-1} at room temperature.

2.3.2 SEM Analysis: The morphology of the CSAC and MCSAC samples were analyzed using the scanning electron microscope (SEM), operated at 15 kV, to determine the changes in the surface microstructures of the activated carbons.

2.4 Preparation of 1000 ppm $Pb(NO_3)_2$ (simulated water) solution

Synthetic wastewater samples were prepared by using analytical grade lead nitrate, $Pb(NO_3)_2$ (99 % Labosi, India) in double distilled water. To prepare 1000 ppm of $Pb(NO_3)_2$, 1.599g of $Pb(NO_3)_2$ was weighed and then dissolved in 100 cm^3 of water and made up to the mark of 1000cm^3 standard volumetric flask to give 1000 ppm $Pb(NO_3)_2$ stock solution. Then Working solutions of 50, 100, 150, and 200 mg/L were prepared from the stock by dilution.

2.5 Batch adsorption experiments

The batch experiments were performed by adding 10 cm^3 each of the various concentration (50, 100, 150 and 200 mg/l) of the stock solution in a set of test tubes containing initial adsorbent dose (1g), pH 6.5, and at temperature 20 ^oC. The solution was shaken using a mechanical Gemmy orbit shaker (model: VRN-480, USA) at 100 rpm for 20 minutes to establish equilibrium condition. After equilibrating, the content of each tube were filtered using a whiteman filter paper and the free ion concentration of lead(II) in the filtrate was measured by flame Atomic Absorption Spectrophotometer FS240AA Agilent U.S.A. at wavelength of 283.3nm using photon hollow cathode lamp system in AAS. The same process was repeated where the Adsorbent dose, contact time, temperature and pH were optimized by continuous variation method (studying one, keeping the other parameters constant). The difference in the lead content before and after adsorption experiments represents the amount of lead adsorbed by the bio-adsorbent.

All experiments were performed at volume (10 cm^3), and 100 rpm. The pH of the original solution and the filtrate solution was determined using HANNA instruments pH meter (pH 209 model, Portugal).

The amount of lead ions adsorbed q_e in mg/l can be expressed as

$$q_e = C_o - C_e \quad (1)$$

Here, The amount of lead ion adsorbed per unit mass of the adsorbent (amount adsorbed in mg/g),q_e and (%) removal was evaluated using the following equations:

$$q_e = \frac{(C_o - C_e)\ V}{W} \quad (2)$$

Where; C_O is the initial ion concentration in mg/l, Ce is the metal ion concentration at equilibrium in mg/l,

V is the volume of metal ion solution in litres, and W is the amount of adsorbent used in gram.

$$\%\ \text{Removal} = \frac{(C_o - C_e)}{C_o}\ X\ 100 \quad (3)$$

2.6 Adsorption isotherms

Adsorption isotherms are mathematical models that describe the distribution of the adsorbate species among liquid and adsorbent, based on a set of assumptions that are mainly related to the homogeneity or heterogeneity of adsorbents [29]. The nature of adsorption was evaluated by fitting the data obtained into Langmuir, Freundlich, Temkin, and Harkins-Jura isotherms, in order to find the best model that represents the equilibrium data for Pb^{2+} adsorption onto MCSAC adsorbent.

2.6.1 Langmuir isotherm: defines a monolayer adsorption on a homogenous surface even at higher adsorbate concentrations. This assumption is expressed mathematical by non linear relation given as:

$$q_e = \frac{q_m K_L C_e}{1 + K_L C_e} \quad (4)$$

Where, q_e is the amountof the Pb(II) ions adsorbed on the MCSAC adsorbent at equilibrium (mg/g), Ce is the equilibrium concentration of the Pb(II) ions in the solution (mg/l), q_m and K_L are the Langmuir constants.

q_m is the maximum monolayer adsorption capacity of the adsorbent (mg/g) and K_L is the energy constant related to the heat of adsorption (related to affinity of binding sites). Equation (4) can be re-arraged in the linear form as;

$$\frac{1}{q_e} = \frac{1}{q_m K_L C_e} + \frac{1}{q_m} \quad (5)$$

q_m and K_L was obtained by plotting $1/q_e$ versus 1/Ce from equation (5). The slope and intercept of the straight line graph gotten gave the values of these constants q_m and K_L as shown in table ….

2.6.2 Freundlich isotherm: defines a multilayer adsorption on a heterogeneous surface of suitable energies. It assumes that heterogenous or different sites with several adsorption energies are involved (non-uniform distribution of sorption heat) [29]. The non linear equation is represented by;

$$q_e = K_f Ce^{1/n} \quad (6)$$

The Freundlich isotherm is represented by the Linear Logarithm equation;

$$\text{Log } q_e = \text{Log } K_f + 1/n \text{ Log Ce} \quad (7)$$

where, q_e is the amount of the adsorbate (Pb^{2+}) adsorbed on the MCSAC adsorbent at equilibrium (mg/g); Ce is the equilibrium concentration of the Pb (II) ions in the solution (mg/l); K_f and 1/n, are the Freundlich constants. K_f is an indicator of adsorption capacity.

2.6.3 Temkin isotherm: Temkin isotherm is used for heterogeneous surface energy system. The linear form is expressed as:

$$q_e = \frac{RT}{b} \ln K_T + \frac{RT}{b} \ln Ce \quad (8)$$

$$q_e = B \ln K_T + B \ln Ce \quad (9)$$

Where, B and K_T are temkin constants, $B = \frac{RT}{b}$ which related to heat of sorption (J/mol), R is gas constant (8.314 $J^{-1}mol^{-1}K$), T is temperature in Kelvin (k) and K_T is the adsorption potential or the equilibrium binding constant (L/g or L/mol) corresponding to the maximum binding energy and interaction between adsorbate and adsorbent [30]. The adsorption data can be analyzed with equation (9). A plot of q_e versus $\ln C_e$ gives the value of constants B and K_T as listed in Table 13.0

2.6.4 Harkins-Jura isotherm: This isotherm accounts for multilayer adsorption and can be explained with the existence of a heterogeneous pore distribution [31]. Harkins Jura adsorption isotherm can be expressed as:

$$\frac{1}{q_e^2} = \frac{B_{HJ}}{A_{HJ}} - \frac{1}{A_{HJ}} \log_{10} C_e \quad (10)$$

Where, A_{HJ} is Harkins-Jura isotherm parameter which accounts for multilayer adsorption and explains the existence of heterogeneous pore distribution, B_{HJ} is the isotherm constants.

2.7 Adsorption kinetics

Kinetic models are time dependent models that can be used to examine the rate of adsorption process and the potential rate-controlling step on the adsorbent surface [32]. To examine the adsorption kinetics of lead (II) ions, the pseudo-first-order and pseudo-second-order were applied to the experimental data.

2.7.1 Pseudo-first-order: The pseudo first order rate equation is one of the most widely used equations for the adsorption of a solute from an aqueous solution and can be expressed in the linear form [33]:

$$\log(q_e - q_t) = \log q_e - \frac{K_1}{2.303}(t) \quad (11)$$

Where q_e and q_t are the amount of metal ion adsorbed (mg/g) at equilibrium and time, t, respectively. K_1 is the first-order reaction rate constant (min^{-1}). A plot of $\log(q_e\text{-}q_t)$ versus t, gives a linear relationship, from which the value of K_1 and q_e can be determine from the slope and intercept [34].

2.7.2 Pseudo-second-order: The linear form of the pseudo second order kinetic rate is given as [35]:

$$\frac{t}{q_t} = \frac{1}{K_2 q_e^2} + \frac{t}{q_e} \quad (12)$$

Where q_e is the amount of adsorbate adsorbed per unit mass of adsorbent at equilibrium (mg/g), q_t is the amount of adsorbate adsorbed at contact time t (mg/g) and K_2 is the pseudo-second-order rate constant ($gmg^{-1}min^{-1}$). A plot of t/q_t versus t gives a linear relationship, from which q_e and K_2 can be determined from the slope and intercept [36].

2.8 Statistical analysis(10 Bold)

Data was analyzed using Microsoft Excel 2007.

III. Results and Discussion

3.1 characterization of activated carbon

In this study, both coconut shell activated carbon (CSAC) and modified coconut shell activated carbon were characterized.

3.1.1 Adsorbent properties

Surface area, bulk and particle density were directly related to the development of porosity of activated carbons. The increase in the ratio of polymer/sample promotes an improvement of the surface area (from 650 m^2/g to 768 m^2/g) and porosity (from 0.635 to 0.688). Porosity varies depending on particle size and aggregation. Porosity decreases as bulk density and particle density increases or vice versa as seen in Table 1.0.

Table 1.0 Physico-chemical characteristics of CSAC and MCSAC

Adsorbent	Bulk density (g/cm^3)	Particle density (g/cm^3)	Surface area (m^2/g)	Porosity	Ash content (%)	Yield (%)
CSAC	0.847	1.333	650	0.635	1.475	50
MCSAC	0.762	2.442	768	0.688	2.092	

3.1.2 Structural morphology

The surface morphology of the activated carbon before and after modification with polymer was evaluated using Scanning electron micrographs (SEM) as shown in figure1.0**a**, **b**. The micrograph showed clearly different surfaces. Fig.1.0a shows that the surface of unmodified activated carbon (CSAC) was rough, irregular and closed with impurities that might be seen from Energy dispersive X-ray (EDX) elemental micro-analysis in fig. 2.0**c**,**d**, and might have contributed to it low porous properties. However, Fig. 1.0b show that modified activated carbon (MCSAC) has improved surface morphology with better porous surface as a result of removal of impurities attached on the surface as seen in EDX elemental table below, which proved that some percentage of metals disappeared from the surface given 95.75 percent atomic concentration of carbon while some such as Tantalum and sodium appeared after modification.

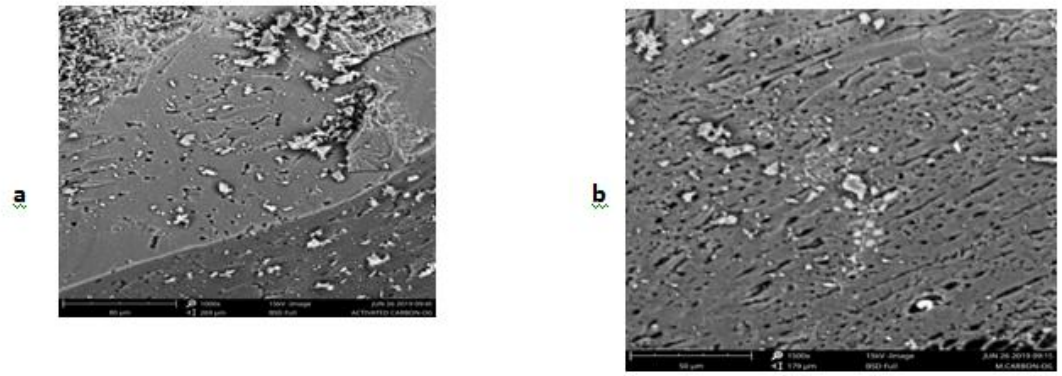

Fig.1.0 SEM image of **(a)** unmodified CSAC and **(b)** modified CSAC

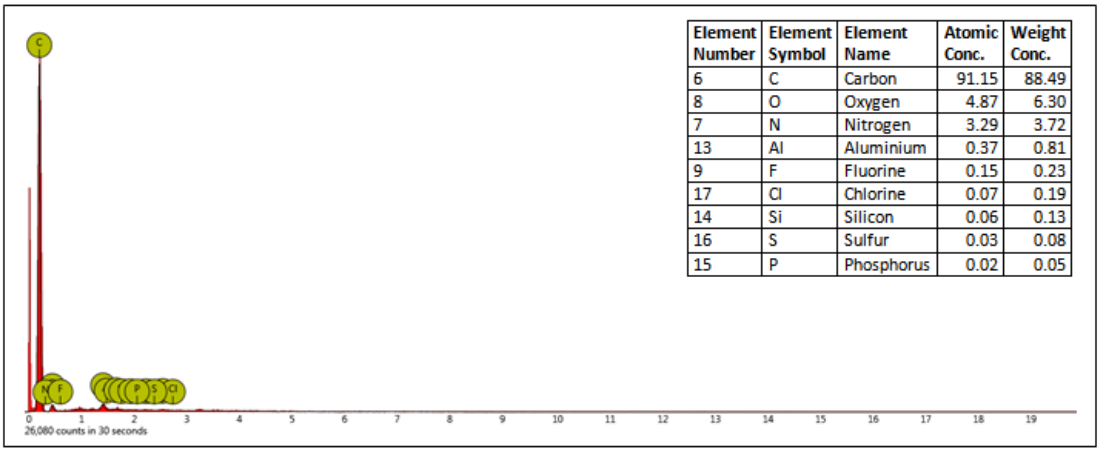

Element Number	Element Symbol	Element Name	Atomic Conc.	Weight Conc.
6	C	Carbon	91.15	88.49
8	O	Oxygen	4.87	6.30
7	N	Nitrogen	3.29	3.72
13	Al	Aluminium	0.37	0.81
9	F	Fluorine	0.15	0.23
17	Cl	Chlorine	0.07	0.19
14	Si	Silicon	0.06	0.13
16	S	Sulfur	0.03	0.08
15	P	Phosphorus	0.02	0.05

Fig. 2.0c: EDX spectra pattern elemental analysis for unmodified -CSAC

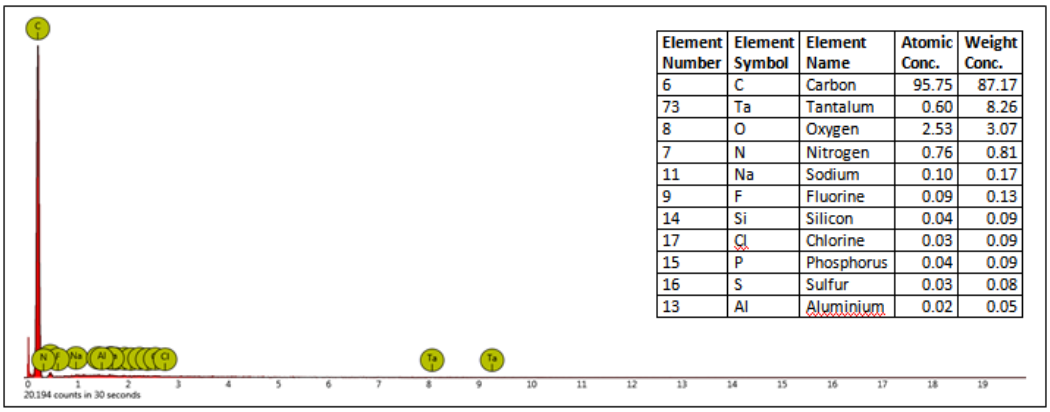

Element Number	Element Symbol	Element Name	Atomic Conc.	Weight Conc.
6	C	Carbon	95.75	87.17
73	Ta	Tantalum	0.60	8.26
8	O	Oxygen	2.53	3.07
7	N	Nitrogen	0.76	0.81
11	Na	Sodium	0.10	0.17
9	F	Fluorine	0.09	0.13
14	Si	Silicon	0.04	0.09
17	Cl	Chlorine	0.03	0.09
15	P	Phosphorus	0.04	0.09
16	S	Sulfur	0.03	0.08
13	Al	Aluminium	0.02	0.05

Fig. 2.0d: EDX spectra pattern elemental analysis of modified-CSAC

3.1.3 FTIR measurements

Fourier transform infrared (FTIR) spectroscopy was used to evaluate the functional groups on the surface of CSAC and MCSAC at frequency regions of 4000 – 600 cm^{-1} as shown in Figure 3.0(e) &(f), and co-added at 32 scans and at 4 cm^{-1} resolution. FTIR spectra were displayed as transmitter values, and several peaks assigned to the vibrations of the CSAC and MCSAC functional groups were detected. Some other ones appeared or added as a result of modification, while some due to wavelength shift in the process. The measurement showed the presence of some functional groups in Table 2.0.

Table 2.0FTIR adsorption bands, functional groups and interpretation for CSAC and MCSAC

Adsorption band (cm-1)		Appearance	Type of vibration	Type of bond	Functional groups
CSAC	MCSAC				
3828.552 - 3592.012	3879.178 - 3632.936	medium, sharp	stretching	O-H	"free" Hydroxyl of carboxylic, alcohols and phenols
3457.103 - 3269.187	3521.839 - 3231.759	strong, broad	stretching	O-H	"intermolecular bonded" Hydroxyl groups
3019.095 - 288.186	3031.678 - 2970.288	Medium	stretching	C-H	assymetric of methyl, methylene and methoxy groups
2751.351	2784.491	Medium	stretching	O=CH	aldehyde with structure -CHO
2601.215	2669.237 - 2522.666	Weak	stretching	S-H	weak stretching thiol
2145.998	2178.303 - 2089.274	Strong	stretching	C≡N	cyanates of nitrile groups
1974.948	1981.481	Medium	stretching	C=C=C	allene
1857.628	1869.205 - 1702.776	Strong	stretching	C=O	ketones, aldehydes, ester, carboxylic groups
1630.752	1609.396	Medium	stretching	C=C	alkene, aromatic ring
1374.225	1388.12 - 1312.86	Strong	stretching	S=O	sulfonyl chloride, sulphonates
1277.913 - 1106.068	1133.473 - 931.543	Strong	stretching	C-O-C, C-O	Stretching vibrations of carbohydrates
841.1585 - 767.8679	727.0389	Strong	bending	C-H, C-Cl	aromatics bonds alkenes and halogeno compound

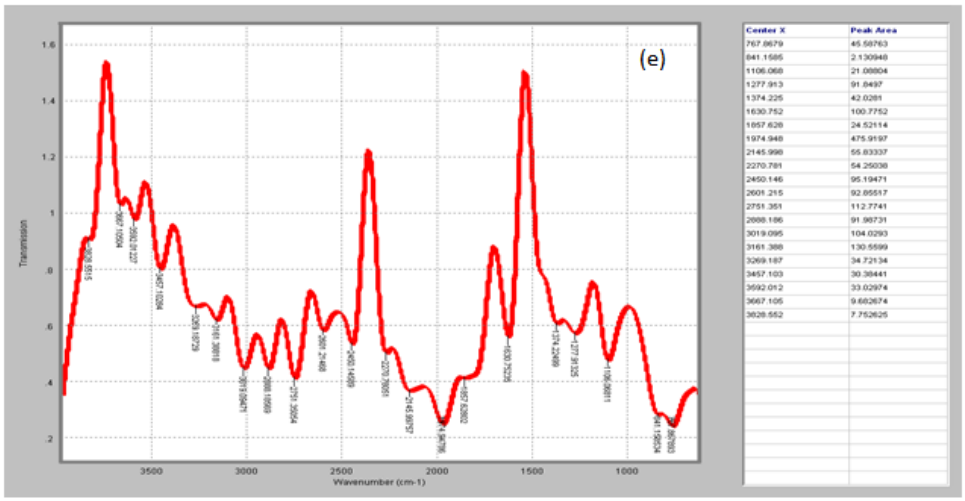

Figure 3.0e FTIR spectrum of CSAC

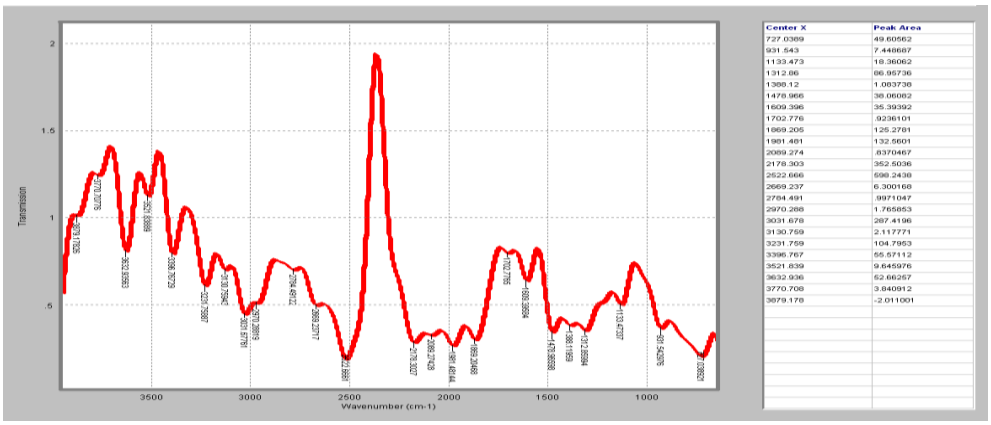

Figure 3.0f FTIR spectrum of MCSAC

3.2 Effect of concentration:

The effect of initial ion concentration on the adsorption efficiency of the MCSAC was studied. Adsorption experiments were carried out at different initial ion concentrations ranging from 50 to 200 mg/l. The percentage of Pb^{2+} removed at 50, 100, 150 and 200 mg/l levels are 62.83, 38.02, 80.63 and 99.07% respectively as seen in Table 3.0. The optimal concentration where high percentage removal were observed was 200 mg/l. It was also observed as a trend that there is an increase of the percentage removal with increase in initial concentration of Pb^{2+} ion. These may be as a result of adequate active sites in the adsorbent even at higher concentrations [39]. Thus, more Pb^{2+} ions were adsorbed from solution at higher concentration level. It is therefore evident that at low concentration, the active sites on the adsorbent surface are not completely covered, so more ions would probably get adsorbed on increase of the initial concentration [40]. Also, from the graph of quantity adsorbed (q_e), between 100 mg/l and 150 mg/l, there is a bit curve seem slow down, it's not a sign of decrease but a sign of sharp increase at higher range of concentration margin which brings about an even increment in the amount adsorbed. The optimal percentage removal and amount adsorbed are 98.78 % and 335.08 mg/g respectively.

Table 3.0: % Removal of the Pb^{2+} at various concentrations, pH 6.5, 100 rpm, 20 min. at 20 ^{o}C using 1.0g of MCSAC adsorbent

Initial Concentration (mg/l)	**Ce**	**% Removal**	**q_e (mg/g)**
50	0.242	62.83	4.09
100	0.326	65.97	6.32
150	0.352	80.63	14.65
200	0.414	98.78	335.08

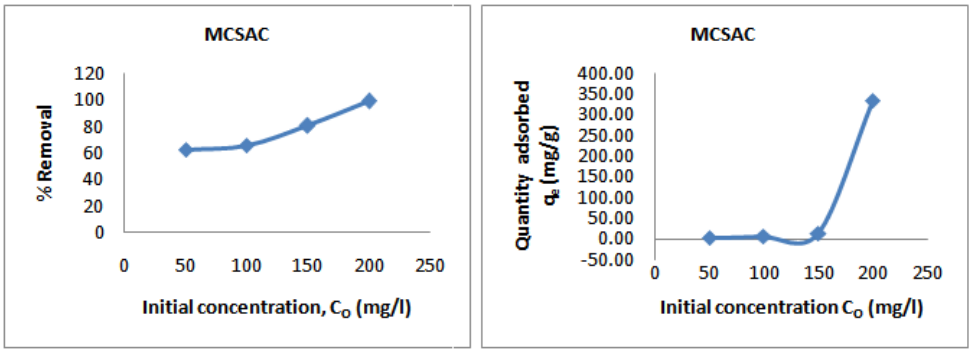

Figure 4.0: Effect of initial Concentration (%Removal and Quantity adsorbed, q_e)

3.3 Effect of contact time

The effect of contact time on the adsorption of Pb^{2+} was studied at different agitation times 5, 10, 15 and 20 min. for Lead concentration of 200 mg/l at room temperature 20 ^oC, pH 6.5 and 100 rpm. Adsorption as a function of time was evaluated in order to determine the equilibrium time required for maximum adsorption of Pb^{2+}. Figure 5.0 show the adsorption of the lead ions using MCSAC. It also showed that the rate of adsorbed Pb^{2+} onto MCSAC was initially rapid and increases as time progresses until it reaches the optimum where the surface coverage of the adsorbent is high at 15 min. and then it slowed down. It is observed that the concentration of lead ions adsorbed on the MCSAC increased with increase in agitation time. This could be due to the migration of higher fraction of Pb^{2+} from the bulk solution through the adsorbent boundary layer onto the active sites of the adsorbent as time progresses [22], or due to the decrease in boundary layer resistance to mass transfer in bulk solution and also increase in kinetic energy of the hydrated Pb^{2+} [22].

Table 4.0: % Removal of the Pb^{2+}at various Contact Time at 20 ^oC using 200mg/l on 1.0 g of MCSAC adsorbent at 100rpm

Contact Time (min)	Ce	% Removal	q_e (mg/g)
5	0.41	98.79	335.12
10	0.40	98.82	335.22
15	0.25	99.26	336.72
20	0.30	99.12	336.22

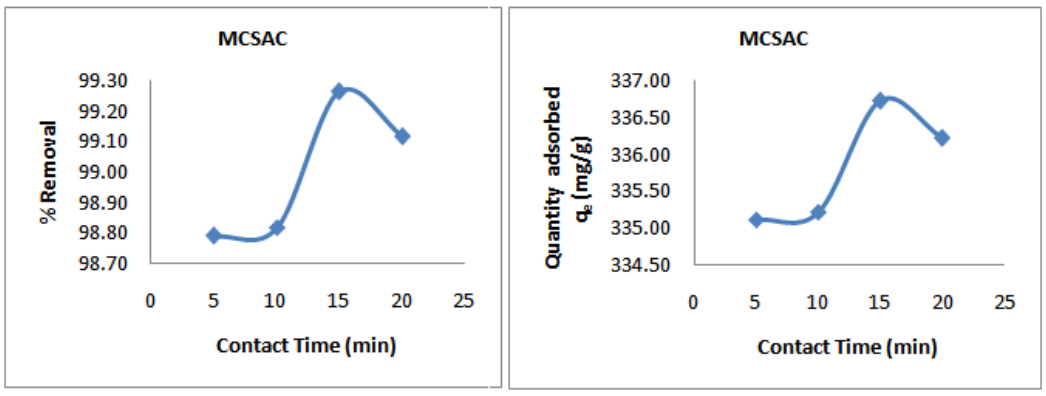

Figure 5.0: Effect of Contact Time (%Removal and Quantity adsorbed, q_e)

3.4 Effect of Adsorbent dose

The effect of adsorbent dosage on the adsorption of Pb^{2+} was studied at various dosages 0.2, 0.4, 0.6 and 0.8 g, keeping other parameters (concentration, time, pH, and temperature) at constant value. From the data obtained, it was observed that with increasing amount of adsorbent, the percentage removal first increases to 99.71% , reaches maximum at 0.2 g and then decreases. Also, Pb(II) uptake (quantity adsorbed or adsorption capacity) q_e decreases as adsorbent dosage increases as shown in Figure 6.0. According to report by Padmavathy [41], at lower adsorbent, concentration number of active sites is still higher, but with the increase in adsorbent dosage, aggregation of particles take place. As a result of that, the efficiency and Pb^{2+} uptake decreases.

Table 5.0 shows the variation of % removal of ions adsorbed with different grams of adsorbent. From the graph, it was clearly observed that the percentage removal and adsorption capacity (q_e) decreased sharply with the increasing of adsorbent dosage. Moreover, the high adsorbent dosage could impose a screening effect of the dense outer layer of the cells, thereby shielding the binding sites from metal [42].

Table 5.0: % Removal of the Pb^{2+}at various Adsorbent Dose at 20 ^oC, using 200mg/l at 100 rpm for 15 min of MCSAC adsorbent

Adsorbent Dose (g)	Ce	% Removal	Quantity Adsorbed (q_e)
0.2	0.10	99.71	1691.10
0.4	0.39	98.85	845.05
0.6	0.13	99.62	563.20
0.8	0.16	99.53	422.03

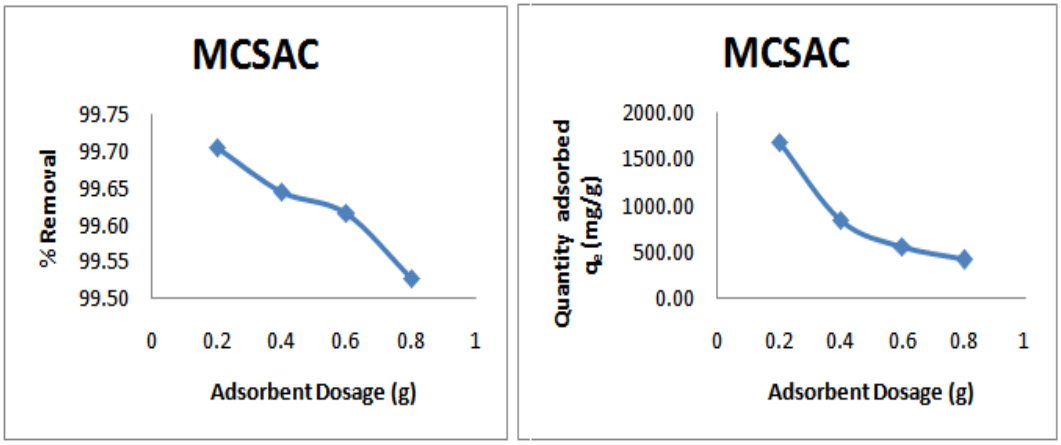

Figure 6.0: Effect of Adsorbent Dose (%Removal and Quantity adsorbed, q_e)

3.5 Effect of temperature

The effect of temperature on the lead adsorption on the adsorbent (MCSAC) was investigated at different temperatures 20^{o}C, 40^{o}C, 60^{o}C and 80^{o}C.The maximum adsorption value for Pb^{2+} solution was 99.51% at 20 ^{o}C as shown in Figure 7.0, it may be due to the initial availability of the active sites, pore size and activation of the adsorbent surface. Also, the adsorption capacity of Pb^{2+} onto MCSAC as seen in figure 7.0 was initially high and decreases as temperature increases until it reaches where the surface coverage of the adsorbent is high at 80^{O}C. In some cases, increase in temperature results in swelling of lignocellulosic material of an adsorbent, thus enabling the large lead molecule to penetrate further which in turn adsorbed in the inner binding sites [43], and may result to an endothermic process.

Table 6.0: % Removal of the Pb^{2+} at various Temperature using 200mg/l at 100 rpm for 15 min of 0.2 g MCSAC adsorbent

Temperature (^OC)	Ce	% Removal	q_e (mg/g)
20	0.167	99.51	1687.75
40	0.211	99.38	1685.55
60	0.632	98.14	1664.50
80	0.800	97.64	1656.10

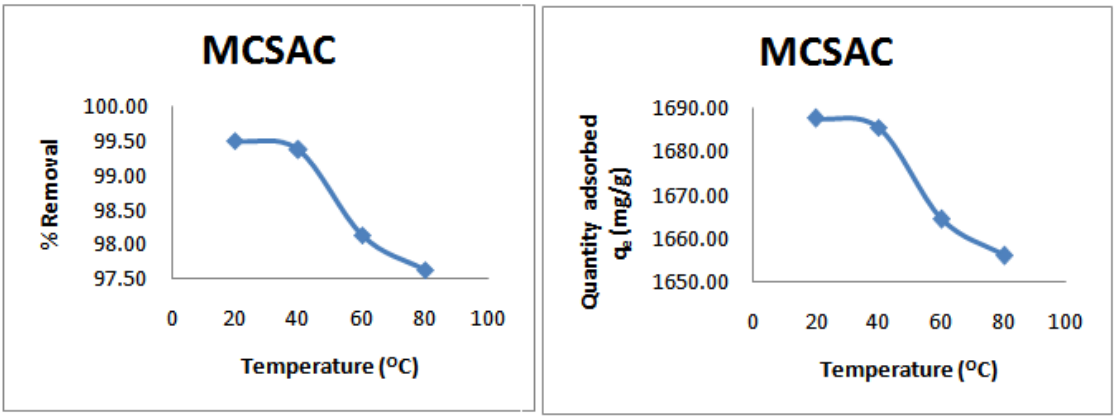

Figure 7.0: Effect of Temperature (%Removal and Quantity adsorbed, q_e)

3.6 Effect of pH

pH is one of the most important factors in controlling the adsorption process. It affects the solubility of the Pb (II) ions concentration of the counter ions on the functional group of the adsorbent and the degree of ionization of the adsorbate during reaction [40]. Thus, the effect of the initial pH value ofthe uptake capacity of MCSAC towards Pb (II) ions was investigated over the pH range 2, 4, 6 and 8, employing the optimal values obtained in the previous experiments which includes 10 ml of the initial Pb (II) ion concentration of 200 mg/l, 0.2 g of adsorbent, 20^{o}C, at 100 rpm for 15min. At initial pH of 2.0, the percentage of Pb^{2+} ions removed was a bit high but decreases with increasing pH, and reached maximum at 95.65%. The variation of the equilibrium uptake of Pb(II) ions with the initial pH value is depicted in Table 7.0, which indicates that the maximum adsorption capacity of MCSAC towards Pb (II) ions (q_e), was 1622.30 mg/g at pH value of 8.0. Which shows that alkaline medium tend to support adsorption more than acidic medium. At low pH values, the surface of the absorbent would be closely associated with hydroxonium ions, by repulsivse forces, to the surface functional groups, consequently decreasing the percentage adsorption of metal [40]. At lower pH value, the H^+ ions compete with the metal cations for the adsorption sites in the system. As the pH increases, the onset of the metal hydrolysis and precipitation begins following the resultant adsorption which occurs before the beginning of hydrolysis [40].

Table 7.0: % Removal of the Pb^{2+} ions at various pH values using 200mg/l at 20 ^{o}C, 100 rpm for 15 min of 0.2g MCSAC adsorbent

PH	Ce	% Removal	q_e (mg/g)
2	6.242	81.60	1384.00
4	8.707	74.33	1260.75
6	12.056	64.46	1093.30
8	1.476	95.65	1622.30

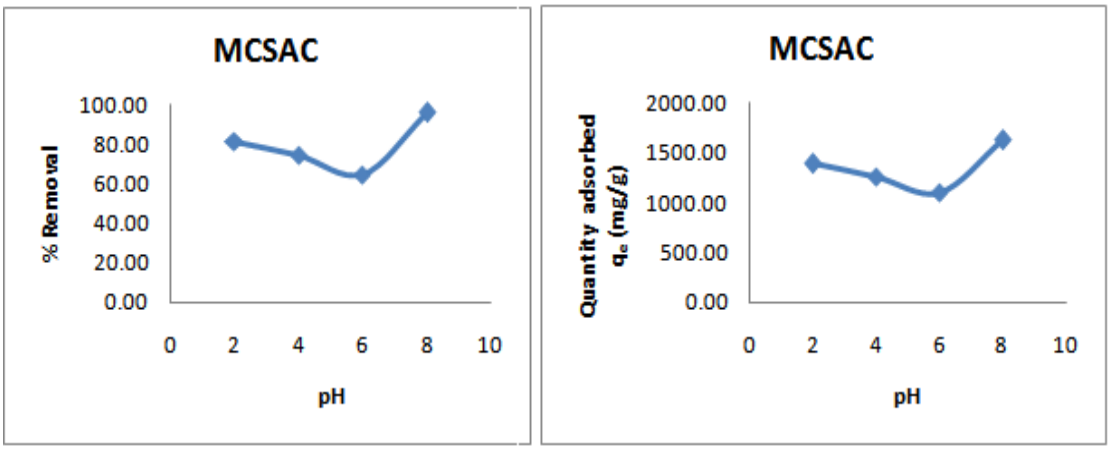

Figure 8.0: Effect of pH (% Removal and Quantity adsorbed, q_e)

3.7 Adsorption isotherms

3.7.1 Langmuir isotherm

Despite the high correlation coefficients (R^2 =0.914) in Langmuir model compare to that of freundlich (R^2 =0.7000) and temkin (R =0.504), the negative slope and the negative which reflected in Langmuir isotherm constants (q_m, K_L and R_L) resulting from the model calculations indicate that this model is inadequate to explain this adsorption process [44, 45, 46]. Also, the essential characteristics of this Langmuir isotherm model can be expressed in terms of a dimentionless separation factor for equilibrium parameter, R_L [47], which is defined as:

$$R_L = \frac{1}{1+K_L C_o} \quad (13)$$

Where, K_L is the Langmuir constant which indicates the nature of adsorption (L/mg), C_o is the initial Pb(II) concentration (mg/l). The separation factor R_L indicates the isotherm shape and whether the adsorption is favourable or not, base on the given criteria; Linear (R_L=1), Unfavourable (R_L>1), Favourable (0<R_L<1), Irreversible (R_L=0) and unfavourable adsorption R_L< 1 [44, 48].

In this work, we evaluated the separation factor R_L for all concentrations to determine whether the adsorption is favourable for the whole range. From Table 8.0, the R_L were found to be -2.0928 to -0.0132 for the initial concentrations of 50 to 200 mg/l Pb (II), and the maximum monolayer coverage capacity (**q_m**) for Pb (II) ions from Langmuir isotherm model was determined to be -3.2154 mg/g, Langmuir isotherm constant (**K_L**) and the separation factor (**R_L**) exhibiting negative values as shown in Table 8.0 and 12.0, indicates that the equilibrium sorption was not favourable, that is R_L<0, and there is a tendency of desorption in the progression.

Table 8.0: Equilibrium experimental datas for Langmuir investigation of Pb (II) ions per unit gram of MCSAC adsorbents.

Initial Concns (mg/l)	Ce	q_e (mg/g)	R_L	$1/q_e$	1/Ce
50	0.242	4.09	-2.0928	0.2445	4.13223
100	0.326	6.32	-0.8512	0.1582	3.06748
150	0.352	14.65	-0.3200	0.0683	2.84091
200	0.414	335.08	-0.0132	0.0030	2.41546

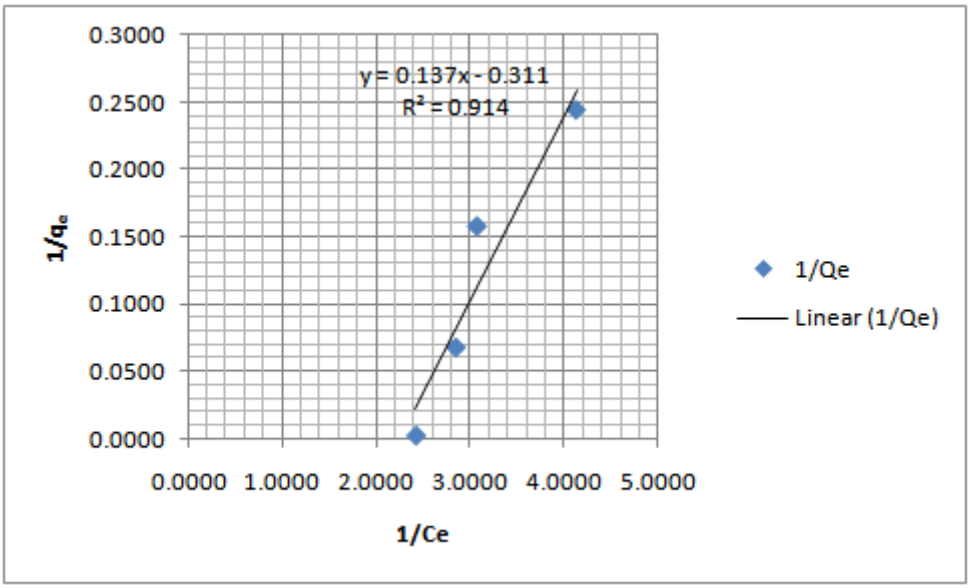

Figure 9.0: Langmuir isotherm plot for adsorption of Pb (II) onto MCSAC

3.7.2 Freundlich isotherm

The ability of Freundlich model to fit the experimental data was examined. Thus, the plot of $\ln q_e$ versus lnCe was employed to generate the intercept value of $\text{Log}K_f$ and the Slope of 1/n. 1/n ranging between 0 and 1 is a measure of adsorption intensity or surface heterogeneity, becoming more heterogenous as its value gets closer to zero [47]. n is an empirical parameter which reflects the effect of concentration on the adsorption capacity and represents the intensity of adsorption that varies with the degree of heterogeneity. The adsorption process is

said to be favourable when the value of n satisfies the condition 1< n <10, otherwise it is unfavourable [45, 48]. As we can see in Table 12.0, the value of n is outside the range of 1–10 indicating unfavourable adsorption process.

Table 9.0: Equilibrium experimental datas for Freundlich investigation of Pb (II) ions per unit gram of MCSAC adsorbents.

Initial Concns (mg/l)	Ce	q_e (mg/g)	log Ce	Logq_e
50	0.242	4.09	-0.6162	0.6117
100	0.326	6.32	-0.4868	0.8007
150	0.352	14.65	-0.4535	1.1658
200	0.414	335.08	-0.3830	2.5251

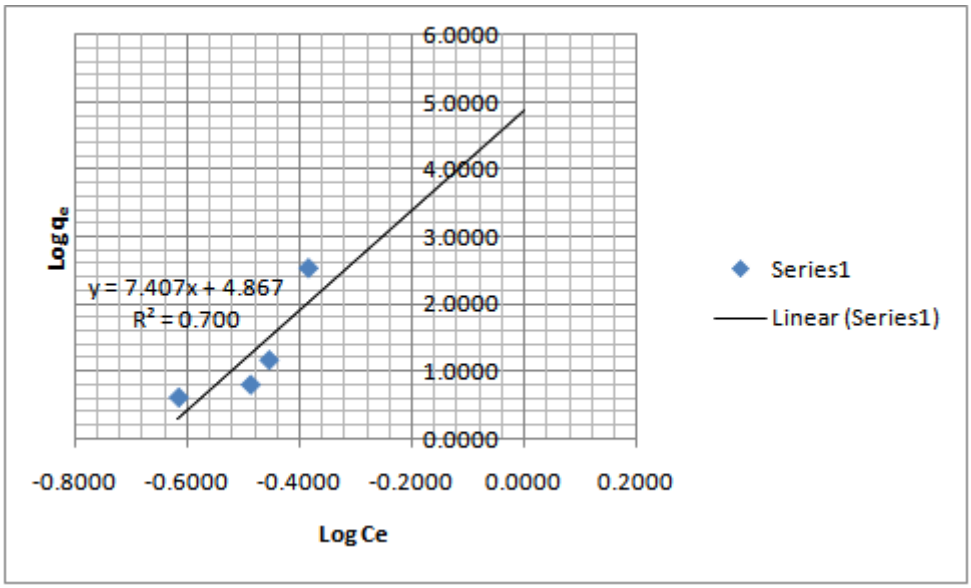

Figure 10.0: Freundlich isotherm plot for adsorption of Pb (II) onto MCSAC

3.7.3 Temkin isotherm

The plot of this isotherm is shown in Figure 11.0. The correlation coefficients R^2 = 0.505 for Temkin isotherm are lower than those of Langmuir and Freundlich isotherm constants. So the adsorption characteristic of Pb^{2+} onto MCSAC cannot be represented by Temkin model..

Table 10.0: Equilibrium experimental datas for Temkin investigation of Pb (II) ions per unit gram of MCSAC adsorbents

Initial Concns (mg/l)	Ce	q_e (mg/g)	lnCe
50	0.242	4.09	-1.4188
100	0.326	6.32	-1.1209
150	0.352	14.65	-1.0441
200	0.414	335.08	-0.8819

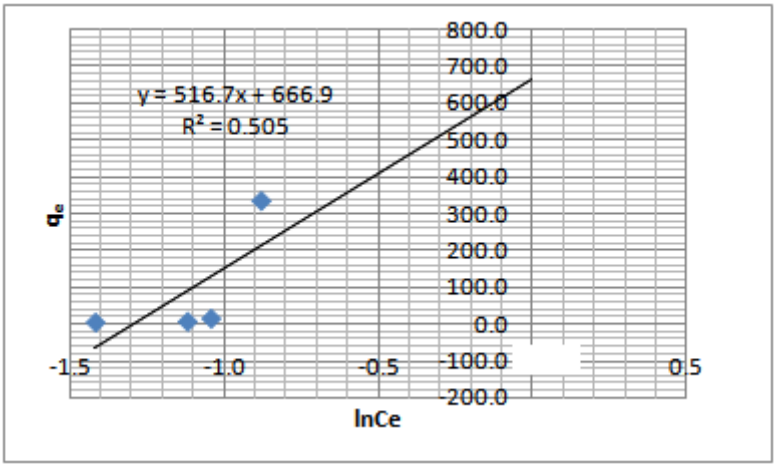

Figure 11.0: Temkin isotherm plot for adsorption of Pb (II) onto MCSAC

3.7.4 Harkins-Jura isotherm

The Harkins-Jura isotherm parameters (A_{HJ} and B_{HJ}) in Table 12.0 were obtained from the slope and the intercept of the plot of $1/q_e^2$ versus logCe respectively [31], as shown in Figure 12.0. The linear correlation coefficient of this isotherm R^2 (= 0.945) showed better fit for the adsorption data than the Langmuir, Freundlich and Temkin isotherms models.

Table 11.0: Equilibrium experimental datas for Harkin-Jura investigation of Pb (II) ions per unit gram of MCSAC adsorbents

Initial Concns (mg/l)	**Ce**	**q_e (mg/g)**	**log Ce**	**$1/q_e^2$**
50	0.242	4.09	-0.6162	0.0598
100	0.326	6.32	-0.4868	0.0250
150	0.352	14.65	-0.4535	0.0047
200	0.414	335.08	-0.3830	0.0000

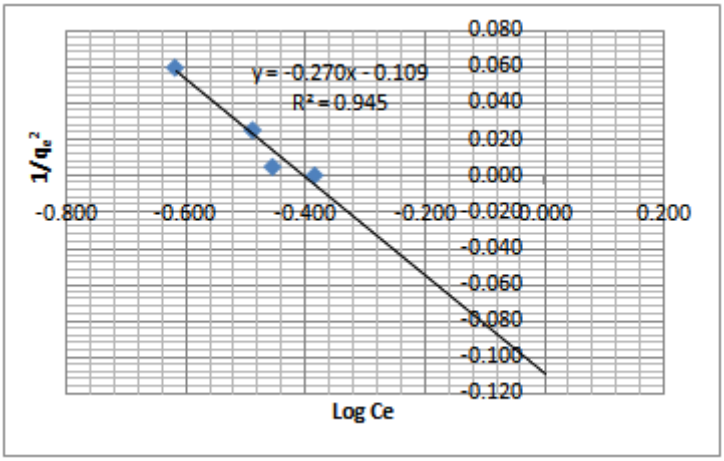

Figure **12.0:** Harkin- Jura isotherm plot for adsorption of Pb (II) onto MCSAC

Table 12.0: Isotherm parameters for Pb^{2+} adsorption onto MCSAC adsorbents

Adsorbent	Langmuir constants			Freundlich constants		
	K_L (L/g)	q_m (mg/g)	R^2	K_f (L/mg)	*n*	R^2
MCSAC	-2.2701	-3.2154	0.9140	73.6207	0.135	0.700
	Temkin constants			**Harkins-Jura constants**		
	K_T (L/g)	B	R^2	A_{HJ}	B_{HJ}	R^2
	3.635	516.7	0.505	3.704	-0.404	0.945

3.8 Adsorption kinetics

From table 13.0, taking negative logarithm of (q_e-q_t) is undefined, and may seem very difficult to obtain since negative differences (values) of equilibrium adsorption capacity (q_e-q_t) between the experiment and calculation was observed, indicating a poor pseudo first-order fit to the experimental data. And examination of the data shows that the pseudo-first-order kinetic model is not applicable to Pb (II) adsorption onto MCSAC. However, Pseudo-second order show greater correlation coefficient R^2=1, this shows the applicability of the second-order kinetic model as seen in Table 14.0 and Figure 13.0.

Table 13.0: Adsorption kinetic parameters for Pb^{2+} adsorption onto MCSAC adsorbent (Co =200 mg/l)

Contact Time, t (min)	q_t (mg/g)	qe (mg/g)	(q_e-q_t) mg/g	t/q_t
5	1675.60	335.08	-1340.52	0.0030
10	1676.10	335.08	-1341.02	0.0060
15	1683.60	335.08	-1348.52	0.0089
20	1681.10	335.08	-1346.02	0.0119

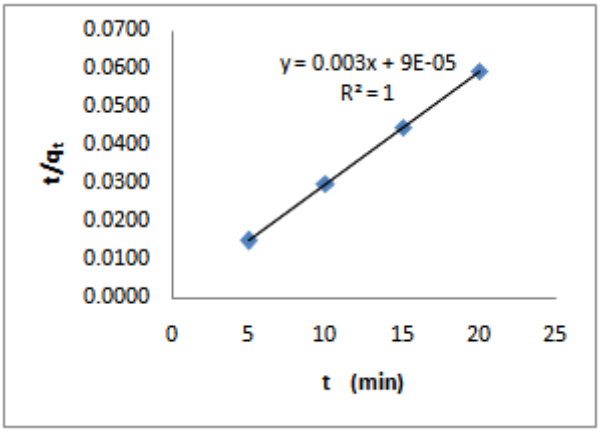

Figure 13.0: Pseudo-Second-Order kinetic plots for the adsorption of Pb(II) onto MCSAC

Table 14.0: Kinetic parameters for Pb^{2+} adsorption onto MCSAC adsorbents

Adsorbent	Pseudo-first-order			Pseudo-second-order		
	K_2	q_e	R^2	K_2 ($gmg^{-1}min^{-1}$)	q_e (mg/g)	R_2
MCSAC	Negative Log (qe – qt) undefine			0.100	333.000	1.000

IV. Conclusion

In this study, introducing inorganic polymer on the activated carbon improves the physical properties of activated carbon, adds more functional groups like amine, carboxyl and hydroxyl group on the surface of the adsorbent [40], as identified by FT-IR analysis. Also, SEM and EDX showed clear image size of the pores and elemental composition of the adsorbent before and after modification. The equilibrium results obtained agreed with the findings that the effectiveness of Pb(II) ion adsorption under optimized conditions (concentration 200 mg/l, contact time 15 min, dosage 0.2 g/10ml, temperature 20 ^{o}C, pH 8) strongly dependent on the quality improvement of the adsorbents. Thus, the result support that coconut shell activated carbon modified with urea immobilized polysiloxane has successfully removed some lead (II) from contaminated water. The amount of metal ion adsorbed increased with increase in concentration and pH of the medium. The isotherms such as Langmuir, Freundlich, temkin and Harkins-Jura models were studied and Harkins-Jura model was found to be in good agreement with experimental data (higher value of coefficients of determination R^2 =0.945). The kinetic study showed the best fitness of pseudo-second-order model on experimental data.

References

[1]. Lenntech Water Treatment Solutions. Heavy , Publish By Lenntech, Rotterdamseweg, Netherlands. (www.lenntech.com/processes/heavy/heavy-metals/heavy-metals.htm), 2004.

[2]. Govind, P. and Madhuri, S. Heavy Metals Causing Toxicity in Animals and Fishes. Research Journal of Animal, Veterinary and Fishery Sciences.2014; 2(2):17-23.

[3]. Caffo, M., Caruso, G., La Fata, G., Barresi, V., Visalli, M., Venza, M. and Venza, I. Heavy Metals and Epigenetic Alterations in Brain Tumors. Current Genomics, 2014; 15:457-463.

[4]. Duruibe, J. O., Ogwuegbu, M. O. C. and Egwurugwu, J. N. Heavy metal pollution and human biotoxic effects. International Journal of Physical Sciences. 2007; 2(5):112-118.

[5]. Mbadcam, J.K., Anagho, S.G., Nsami, J.N., and Kammegne, A.M. Kinetic and equilibrium studies of the adsorption of lead (II) ions from aqueous solution onto two Cameroon clays: Kaolinite and smectite. Journal of Environmental Chemistry and Ecotoxicology. 2011; 3(11):290-297.

[6]. Zamzow .M., Eichbau .B., Sandgren .K., Shanks .D. Removal of Heavy Metals and Other Cations from Wastewater Using Zeolites. Sep. Sci. Technol.(1990); 25(13-15):1555-1569.

[7]. WHO (2018). Lead Poisoning and Health. World Health Organization. (https://www.who.int/news-room/fact-sheets/detail/lead-poisoning-and-health).

[8]. Masindi, V. and Muedi, K.L., Environmental Contamination by Heavy Metals. Intechopen. 2018; 115-133.

[9]. Eruola, A.O and Ogunyemi, I.O. Evaluation of the Adsorption Capacity of the Coconut Shell and Palm-Kernel Shell Adsorbents Powder for the Sorption of Cadmium (11) Ions from Aqueous Solution. IOSR Journal of Environmental Science, Toxicology and Food Technology. 2014; 8(6): 55-63.

[10]. Mandina, S., Chigondo F., Shumba, M., Nyamunda, B.C. and Sebata, E. Removal of chromium (VI) from aqueous solution using chemically modified orange (citrus cinensis) peel. IOSR Journal of Applied Chemistry. 2013; 6(2):66-75.

[11]. Uddin, M.K. A Review On The Adsorption of Heavy Metals By Clay Minerals, With Special Focus On The Past Decade. Chemical Engineering Journal. 2016; 308:438-462.

[12]. Khan, M.A., Uddin, M.K., Bushra, R., Ahmad, A., Nabi, S.A. Synthesis and characterization of polyaniline Zr (IV) molybdophosphate for the adsorption of phenol from aqueous solution, React. Kinet. Mech. Catal. 113 (2014) 499–517.

[13]. Gupta, V.K., Kumar, R., Nayak, A., Saleh, T. A. and Barakat, M.A. Adsorptive removal of dyes from aqueous solution onto carbon nanotubes: a review, Adv. Colloid Interface Sci. 2013; 193: 24–34.

[14]. Saha, S.N. and Mondal, R. Activated Carbon From Coconut Shell By Using Pyrolysis and Fluidized Bed Reactors. Access from www.academia.edu.(no date).

[15]. Aderibigbe, A.D., Ogunlalu, O.U., Oluwasina, O.O. and Amoo, I.A., Adsorption studies of Pb^{2+} from aqueous solutions using unmodified and citric acid-modified plantain (musa paradisiacal) peels. IOSR journal of applied chemistry. 2017;10(2):30-39.

[16]. Onundi, Y. B., Mamun, A. A., Al Khatib, M. F., Ahmed, Y.M. Adsorption of copper, nickel and lead ions from synthetic semiconductor industrial wastewater by palm shell activated carbon. Int. J. Environ. Sci. Tech. 2010; 7 (4):751-758.

[17]. Hajji, S. and Mzoughi, N. Kinetic, equilibrium and thermodynamic studies for the removal of lead ions from aqueous solutions by using low cost adsorbents: a comparative study. IOSR Journal of Applied Chemistry, 2018; 11(7):12-24.

[18]. Nwosu, F.O., Olu-Owolabi, B.I., and Adebowale, K.O. Kinetics And Thermodynamic Adsorption Of Pb (II) And Cd (II) Ions From Used Oil Onto Thevetia Neriifolia Nutshell Active Carbon. Current Research in Chemistry. 2012; 4(2):26-40.

[19]. Thajeel, A.S. Isotherm, Kinetic and Thermodynamic of Adsorption of Heavy Metal Ions onto Local Activated Carbon. Aquatic Science and Technology. 2013;1(2): 52-77.

[20]. Abdulkarim, M. and Abu Al-Rub, F., Adsorption of Lead Ions from Aqueous Solution onto Activated Carbon and Chemically-modified Activated Carbon Prepared from Date Pits. Adsorption Science and Technology. 2003; 22(2):119-134.

[21]. Kumar.P.S., Vincent . C., Kirthika. K. and Kumar, K.S. Kinetics And Equilibrium Studies Of Pb^{2+} Ion Removal From Aqueous Solutions By Use Of Nano-Silversol-Coated Activated Carbon. Brazilian Journal of Chemical Engineering. 2010; 27(2):339-346.

[22]. Haghdoost,G., Aghaie, H. and Monajjemi, M., Investigation of Langmuir and freundlich adsorption isotherm of Pb2+ ions by micro powder of cedar leaf.Journal of Physical and Theoretical Chemistry. 2016; 13 (3): 289-296.

[23]. Jahangard, A., Sohrabi, M., and Beigmohammadi, Z. Sorption of Lead (II) Ions on Activated Coconut Husk. Iranian Journal of Toxicology. 2016; 10(6):23-29.

[24]. Goel, J., Kadirvelu, K., Rajagopal, C. and Garg, V. K. Removal of lead(II) by adsorption using treated granular activated carbon: Batch and column studies. Journal of Hazardous Materials. 2005; B125: 211–220.

[25]. Song, C., Wu, S., Cheng, M., Tao, P., Shao, M. and Gao, G. Adsorption Studies of Coconut Shell Carbons Prepared by KOH Activation for Removal of Lead(II) From Aqueous Solutions. Sustainability. 2013; 6,86-98.

[26]. Samiey, B., Cheng, C. H. and Wu, J. Organic-Inorganic Hybrid Polymers as Adsorbents for Removal of Heavy Metal Ions from Solutions: A Review. Materials.2014; 7:673-726.

[27]. Sener, S., Erdemoglu, M., Asilturk, M., and Sayilkan, H. The Effect Of Silane Modification On The Adsorptive Properties of Natural Pyrophylite and Synthetic Titanium-Based Powders Prepared by The Sol-Gel Process. Turk. J. Chem. 2005; 29:487-495.

[28]. Ezeh E.C., Ukoha P.O., Bulus H., Nweze B.N., Nwagu N.I., Nsude P.O., and Agboeze E., Adsorption isotherms and kinetic studies of Pb2+ and Cu2+ sorption by semicarbazide immobilized polysiloxane as material for water purification. A publication of Chemical Society of Nigeria, Anachem Journal. 2019; 9(1)

[29]. Kumar, S.P., Vincent, C., Kirthika, K.and Kumar, S.K., Kinetics and equilibrium studies of Pb2+ ion removal from aqueous solutions by use of nano-silversol-coated activated carbon. Brazilian Journal of Chemical Engineering. 2010; 27(2):339-346.

[30]. Piccin, J.S., Dotto, G.L. and Pinto, L.A.A., Adsorption isotherms and thermochemical data of FD&C red N^{O} 40 binding by chitosan.Brazilian Journal of Chemical Engineering. 2011;28(2):295-304.

[31]. Oladoja, N.A., Ololade, I.A., Idiaghe, J.A. and Egbon, E.E., Equilibrium isotherm analysis of the sorption of congo red by palm kernel coat. Central European Journal of Chemistry. 2009; 7(4):760-768.

[32]. Kocer, N.N., Uslu, G. and Cuci, Y., The adsorption of Zn(II) ions onto chitin: determination of equilibrium, kinetic and thermodynamic parameters. Adsorption Science and Technology. 2008; 26(5): 333-344.

[33]. Lagergren, S., About the theory of so-called adsorption of soluble substances. K. Sven. Vetenskapsakad.Handlingar Band. 1898; 24: 1-39.

[34]. Pathania, D.,Sharma, S. and Singh, P., Removal of methylene blue by adsorption onto activated carbon developed from Ficuscaricabast. Arabian Journal of Chemistry. 2017;10:1445-1451.

[35]. Ho, Y.S. , Mckay, G., Wase, D.A.J. and Forster, C.F. Study Of The Sorption Of Divalent Metal Ions On To Peat. Adsorption Science and Technology. 2000; 18(7):639-650.

[36]. Bhattacharyya, K.G., Sharma, A., Kinetics and thermodynamics of methylene blue sorption on neem (Azadirachtaindica) leaf powder. Dyes and Pigments. 2005; 65: 51-59.

[37]. Rehman, R., Abbas, A., Murtaza, S., Anwar, J., Mahmud, T., and Akbar, S., Adsorption parameters optimization for removal of alizarin red-S and brilliant blue FCF dyes from water using Abelmoschusesculentus stem powder. Journal of Chemical Society of Pakistan. 2013;35(2):443-448.

[38]. Hameed, B.H., Ahmad, A.A. and Aziz, N. Isotherm, Kinetics And Thermodynamics Of Acid Dye Adsorption On Activated Palm Ash. Chemical Engineering Journal. 2007; 133(1-3):195-203.

[39]. Abdulsalam, M., Che Man, H., Idris, A.I., Abidin, Z.Z., and Yunos, K.F., The pertinence of Microwave Irradiated Decolourization: Structural Morphology and Adsorption Optimization Using the Response Surface Method (RSM). International Journal of Environmental Research and Public Health. 2018;15:1-19

[40]. Anierobi, P. O. (2014). Modification of Coconut shell Activated Carbon with an Azo ligand for the removal of Cd^{2+}, Pb^{2+} and Ni^{2+} from polluted water. A Masters project submitted to the department of Industrial Chemistry, Faculty of Physical Sciences, University of Nigeria, Nsukka.

[41]. Padmavathy, K.S., Madhu, G. and Haseena, P.V., A study on effects of pH, adsorbent dosage, time, initial concentration and adsorption isotherm study for the removal of hexavalent chromium (Cr (VI)) from wastewater by magnetite nanoparticles. Procedia technology. 2016;24:585-594.

[42]. Tumin, N.D., Chuah, A.L., Zawani, Z. and Rashid, S.A. Adsorption Of Copper From Aqueous Solution By Elais Guineensis Kernel Activated Carbon. Journal of Engineering Science and Technology. 2008; 3(2):180-189.

[43]. Rehman, R., Abbas, A., Murtaza, S., Anwar,. J., Mahmud, T. and Akbar, S. Adsorption Parameters Optimization For Removal Of Alizarin Red-S And Brilliant Blue Fct Dyes From Water Using Abelmoschus Esculentus Stem Powder. Journal of Chemical Society of Pakistan. 2013; 35(2):443-448.

[44]. Bicer, G. and Gonen, F., Telon Blue AGLF Adsorption by NiO-Based Nanomaterials: Equilibrium, Kinetic, and Thermodynamic Approach. Journal of the Turkish Chemical Society, 2017;4(3):675-690.

[45]. Alsenani G. Studies On adsorption of crystal violet dye from aqueous solution onto calligonum comosum leaf powder (CCLP). Journal of American Science. 2013;9(8):30-35.

[46]. Alshabanat M., Alsenani G., and Almufariji R. Removal of crystal violet dye from aqueous solutions onto date palm fiber by adsorption technique. Journal of chemistry. 2013; 1-6.

[47]. Okoli, J.U. and Ibe, E., Adsorption studies of heavy metals by low-cost adsorbents. Journal of Applied Science and Environmental Management. 2014; 18(3):443-448.

[48]. Ibrahim, M.B. and Sani, S., Comparative isotherms studies on adsorptive removal of congo red from wastewater by watermelon rinds and neem-tree leaves. Open journal of physical chemistry. 2014;4:139-146.

Ogbeide Osareme .M" Isotherms, kinetics and equilibrium Studies of adsorption of Lead (II) ions from aqueous solutions Using Polymer-Modified Coconut Shell Activated Carbon (MCSAC)" IOSR Journal of Environmental Science, Toxicology and Food Technology (IOSR-JESTFT) 13.8 (2019): 28-43.